Theoretical study of structural, electronic, and optical properties of Zn_mSe_n clusters

Biplab Goswami,[1] Sougata Pal,[1] Pranab Sarkar,[1,*] G. Seifert,[2] and M. Springborg[3]

[1]*Department of Chemistry, Visva-Bharati University, Santiniketan -731235, India*
[2]*Institute for Physical Chemistry and Electrochemistry, Technical University of Dresden, 01062, Dresden, Germany*
[3]*Physical and Theoretical Chemistry, University of Saarland, 66123 Saarbrücken, Germany*

We present density-functional theoretical results of structural, electronic, and optical properties of ligand-free Zn_mSe_n clusters as a function of size of the cluster. We have optimized the structure, whereby our initial structures are spherical parts of either zinc blende or wurtzite crystal structure and we have studied systems up to almost 200 atoms. The calculations were performed by using density-functional tight-binding (DFTB) method. The results include the radial distribution of atoms and of Mulliken populations, the electronic energy levels (in particular the highest occupied molecular orbital and lowest unoccupied molecular orbital), the band gap and the stability as a function of size and composition. In addition to structural and electronic properties we present electronic excitation spectra obtained from time-dependent density functional response theory.

I. INTRODUCTION

During the last couple of decades, semiconductor quantum dots (QDs) have attracted much attention not only for a variety of new interesting physical and chemical properties but also for their potential applications.[1–4] When their size approaches the exciton Bohr radius, QDs exhibit new properties that differ dramatically from those of the bulk material. The special properties may be explained through what is commonly known as quantum size effects. One result of quantum size effects is the tunable band gap as a function of size of the nanocrystallite. The ability to use size as a variable in tailoring the desired properties of the system have made semiconductor QDs promising materials for the development of new electronic and optical devices such as light emitting diodes, solar cells, nanosized switching devices etc.[5–9] II-VI semiconductor materials are particularly interesting in this regard and have been the focus of many experimental and theoretical investigations in recent years.[10–25] Among II-VI semiconductors, zinc selenide based materials have a special importance and has been intensively studied since the 1970s. The ZnSe based photonic devices, such as the saturable-absorber Q switch,[26] blue-ultraviolet photodetector,[27] blue-green laser diode,[28] and modulated waveguide[29] have been realized recently. Though the ZnSe QDs have been well investigated experimentally,[26–33] theoretical studies of its electronic structure and optical properties are very scarce.[34] To the best of our knowledge, the only known theoretical investigation on ZnSe clusters are by Deglmann *et al.*[34] who, however, studied only small ZnSe clusters up to a heptamer from which it is very difficult to extract information about size dependence.

Theoretical investigation of semiconductor nanostructures is of crucial importance since it allows one to both investigate fundamental physics and to optimize nanostructured devices. The advantage of theoretical studies is that the system is well defined and that properties beyond those that are experimentally available can also be examined. The disadvantage is that the systems may be unrealistic, that one in most cases has to make more or less realistic assumptions on the

structure, the interactions with, e.g., ligands, a solvent, and other nanoparticles are not included, and that kinetic effects are not taken into account. Thus, rather than replacing experiment, theory offers a useful complementary approach to explore the properties of nanoparticles.

However, theoretical studies of nanoclusters with a large number of atoms are computationally very demanding and hence to study the clusters of larger size one has to restore various approximations. With accurate parameter-free methods one has to consider either very few sizes and structures for which, furthermore, a certain symmetry may be assumed. Alternatively, when studying a whole class of size and/or structures, also of low symmetry, less accurate methods are better suited. These include the effective mass approximation method, pseudopotential method, tight-binding approximation based method, etc.[34–42] In the present paper we have employed density-functional tight-binding (DFTB) method[43,44] to study the structural and electronic properties of both stoichiometric and nonstoichiometric Zn_mSe_n clusters for $n+m$ approximately equal to 200. We shall investigate how the different structural, electronic properties, viz., radial distribution of atoms, Mulliken populations, density of states, and spatial dependence of highest occupied molecular orbital (HOMO) and lowest unoccupied molecular orbital (LUMO) change as a function of size. By analyzing the optimized geometry we shall seek to identify which atoms are close to the surface. This is an important issue because the surface is that part of the system that will interact with any other system and because it gives indirect information about how to modify the system properties by adding surfactants. In addition we shall study the electronic excitation spectra of stoichiometric ZnSe clusters using time-dependent density functional response theory.[45]

We have considered spherical parts of both zinc blende and wurtzite crystals. By putting the center of the sphere on the midpoint of a Zn-Se bond, stoichiometric Zn_nSe_n clusters are obtained, whereas we obtain nonstoichiometric Zn_mSe_n clusters by placing the center on an Zn or a Se atom. After the initial structures were defined as described above, the structure was allowed to relax to its nearest local total-energy

minimum. In analyzing the results, we considered both the initial and final structures, whereby the effects of structural relaxations could be identified.

The article is organized as follows. In Sec. II we briefly mention the density functional method as used in the present work. We devote Sec. III to present and discuss the results of our calculation on various finite clusters. Section IV contains a brief summary of our findings.

II. THEORETICAL METHOD

The calculational electronic-structure method used in this study, the density-functional tight-binding method (DFTB) has been described in detail elsewhere.[43,44] The density-functional tight-binding method has also been used for the structural optimization of the clusters.[46–50] The DFTB method is a parametrized DFT scheme based on expanding the solutions to the Kohn-Sham (KS) equations in a basis set of Linear combination of atomic orbitals (LCAO). The LCAOs were obtained from self-consistent, local-density-approximation calculations on the isolated, neutral atoms using a large set of Slater-type orbitals. For the system of interest, the effective one electron potential in the KS Hamiltonian is approximated by a superposition of the atomic potentials of the corresponding neutral, noninteracting atoms. Furthermore, only two-center Hamiltonian matrix elements are considered. The total energy is written as the sum of all occupied Kohn-Sham energies which represents the "band-structure" energy and the repulsive two-center terms between the atoms located at R_j and R_k as follows:

$$E = \sum_i^{occ} \epsilon_i + \frac{1}{2}\sum_j \sum_{k \neq j} U_{jk}(|\vec{R}_j - \vec{R}_k|). \tag{1}$$

The pair potentials U_{jk} are determined so that the total energy curves of the diatomics are well reproduced. To test its transferability to larger systems we first performed calculations on infinite, periodic, crystalline structures. This led to optimized lattice constants for the zinc-blende structure of 5.61 Å, for the wurtzite structure of 4.02 and 6.57 Å. The experimental values for the zinc-blende and wurtzite structures are 5.67, 3.98, and 6.53 Å, respectively.[51] Thus the structural parameters of the infinite crystalline material are well produced. The total energy difference between the wurtzite and zinc-blende structures is found to be very small 4.3 meV/atom with the zinc-blende structure being the stabler one. As a further test of the accuracy we also calculated the bulk moduli for the two crystal structures. We found 84, 76 GPa for zinc-blende and wurtzite structures, respectively. The experimental[51] value for zinc blende is 77.1 GPa, i.e., in good agreement with our value. The good agreement makes us believe that the approach is accurate and the results for finite clusters are accurate, too.

Furthermore, we used an extension performing within time-dependent (TD) density-functional response theory (DFRT)[45] for the calculation of the excitation spectra. The calculations performed by this program package are referred to as TD-DFRT-TB. It was previously used for the calculation of optical properties of CdS clusters.[52]
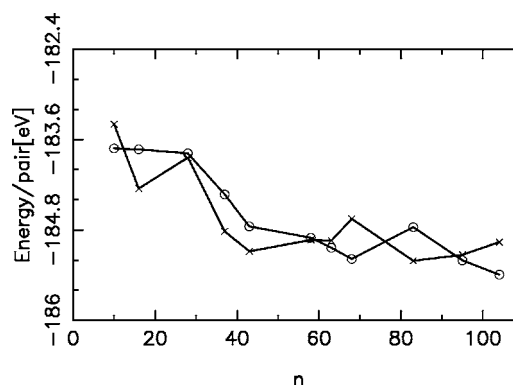

FIG. 1. Variation in the total energy per ZnSe pair for stoichiometric Zn_nSe_n clusters as function of n for (crosses) zinc-blende and (circles) wurtzite derived clusters.

For the calculations presented here, all electrons except for the $4s$ and $3d$ electrons of zinc and the $4s$ and $4p$ electrons of selenium were treated within a frozen core approximation. Now to make sure that the optimized structures we obtained are not of saddle point we carried out harmonic analysis for small clusters (e.g., $Zn_{10}Se_{10}$, both zinc-blende and wurtzite structure). The lowest vibrational frequencies calculated are 273 and 292 cm^{-1} for zinc-blende and wurtzite modification of $Zn_{10}Se_{10}$ clusters, respectively. For larger clusters we have ascertained this in two ways. First, for each structure, we made a small random displacement in each direction for each atom and let the structures relax again. In relaxation the perturbed structure returns to the starting point. Secondly, for each cluster we have generated several initial geometries and most of them in optimization leads to the same minimum.

III. RESULTS AND DISCUSSIONS

A. Stoichiometric clusters

In Fig. 1 we have shown the variation in the total energy per Zn_nSe_n pair as a function of cluster size for clusters derived from zinc-blende and wurtzite crystal structures. The figure shows that the relative stability of the zinc-blende and wurtzite derived clusters varies as a function of cluster size. The total energy difference is significantly larger than the corresponding value for the infinite systems. This finding was also observed for CdS, InP, CdSe, and ZnS clusters.[46–50] The interesting point to note here is that the question which structure is more stable for a given size not only depends on size but also on the material (i.e., the curves for ZnS, CdS, InP, CdSe, and ZnSe are different). There are also experimental evidences that the structure of the clusters can switch between wurtzite and zinc-blende depending on the size.[53]

In describing the structural properties of the clusters we shall discuss the radial distribution of atoms thereby focus on Zn and Se atoms and, moreover, compare unrelaxed and relaxed clusters. The initial, unrelaxed structures are finite, spherical parts of zinc-blende and wurtzite crystal structures with the center at an Zn-Se nearest-neighbor bond. In order to analyze the structure we first define the center of the Zn_mSe_n cluster through
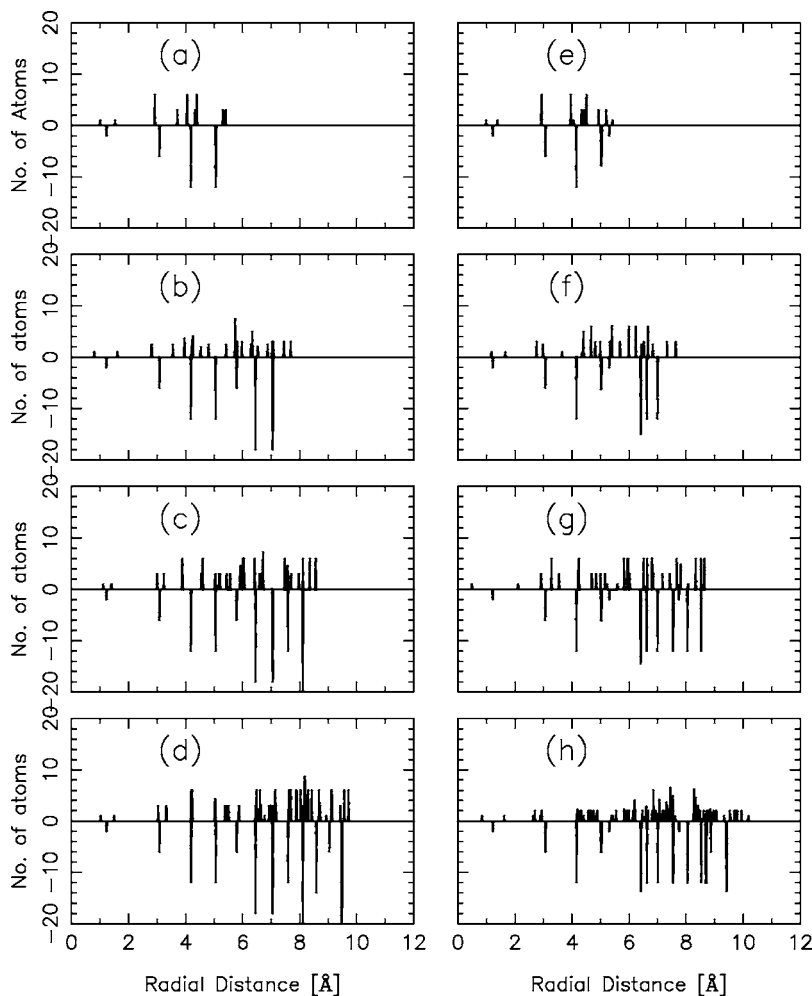
FIG. 2. Radial distribution of zinc and selenium atoms for zinc-blende (left column) and wurtzite-derived clusters (right column) of different sizes: (a),(e) $Zn_{16}Se_{16}$; (b), (f) $Zn_{37}Se_{37}$; (c),(g) $Zn_{58}Se_{58}$; and (d),(h) $Zn_{83}Se_{83}$. In each panel, the upper part is representing the relaxed and the lower part the unrelaxed structure, respectively.

$$\vec{R}_0 = \frac{1}{n+m} \sum_{j=1}^{n+m} \vec{R}_j, \qquad (2)$$

where the summation goes over all the atoms of the cluster. Subsequently the radial distance for the jth atom is defined as

$$r_j = |\vec{R}_j - \vec{R}_0|, \quad j = 1, 2, \ldots, n+m. \qquad (3)$$

Figure 2 shows the radial distributions of eight different stoichiometric clusters with either zinc-blende (left column) or wurtzite structure (right column). The figure shows the radial distances for both zinc and selenium atoms of the optimized structure (upper half) and of the initial geometry (lower half). In general we see that the structural relaxations are almost throughout the whole region of the clusters with a somewhat larger relaxation in the outer region. In this region, some atoms move away from the center of the cluster, whereas others approach the center. Inspecting the radial distribution of the zinc and selenium atoms separately (not shown) it is found that, in the outer parts, only selenium atoms move outward whereas the zinc atoms move inward. Zinc, being a typical metal atom, prefers a high coordination, whereas selenium atom prefers a low coordination. This different behavior of chalcogen and metal atoms are also found for CdS, CdSe, and ZnS clusters.[46,49,50] Many studies concerning theoretical and experimental surface studies of II-VI semiconductor compounds show the same kind of surface relaxation: anions relax outward and the cations relax inward.

Turning to the electronic properties of the clusters, we show in Fig. 3 the Mulliken gross populations for the individual atoms as a function of their radial distance of Eq. (3). Only the valence electrons are included, i.e., for the neutral atoms these numbers would be 12 for Zn and 6 for Se. It is readily seen from this figure that in the inner part of the clusters there is a small electron transfer from Zn to Se which is largely independent of the radial distance, whereas in the outer region we can define a surface region characterized by an increased electron transfer and having thickness of about 2.5–3.5 Å, essentially independent of size of the cluster and of whether it has been derived from the zinc-blende or wurtzite crystal structure. Also this finding is in accord with our previous results for CdSe clusters.[49] Finally a careful inspection of Fig. 3 reveals that the outermost atoms are Se as mentioned above.

In Fig. 4 we have shown the density of states, obtained by broadening the individual electronic states slightly with Gaussian for four representative systems of increasing size for clusters of zinc-blende and wurtzite derived structures. It is observed that the states below the Fermi energy tend to
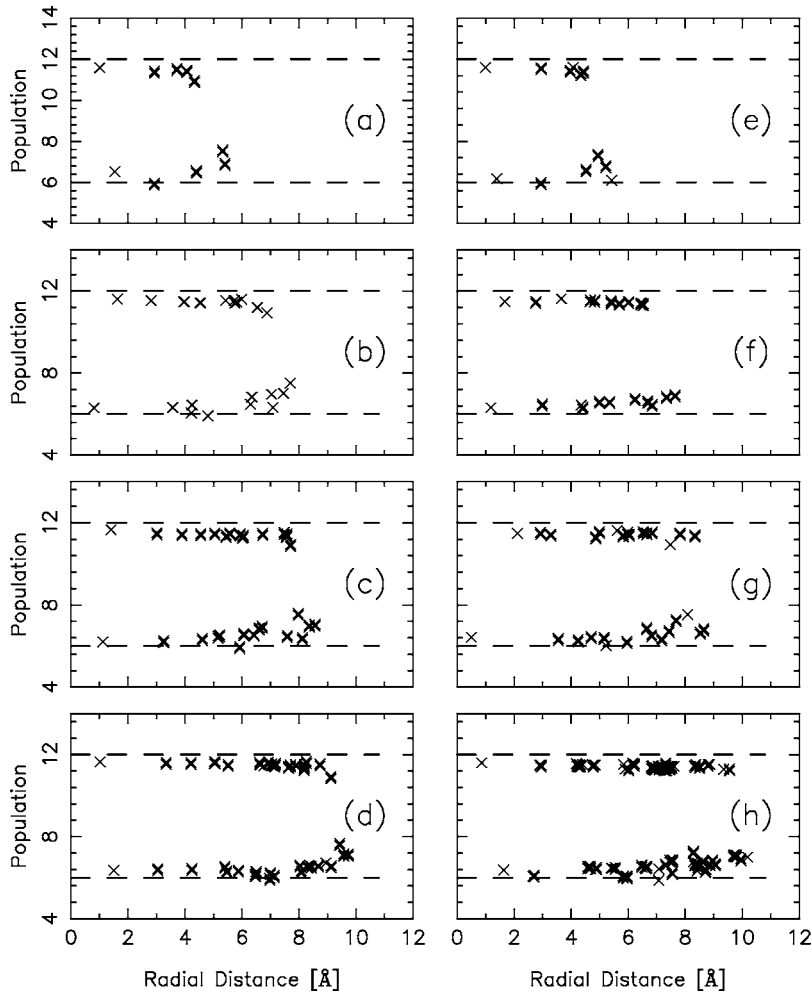
FIG. 3. Radial distribution of Mulliken gross populations for the valence electrons of Zn and Se atoms for zinc-blende (left column) and wurtzite-derived clusters (right column) of different sizes: (a),(e) $Zn_{16}Se_{16}$; (b),(f) $Zn_{37}Se_{37}$; (c),(g) $Zn_{58}Se_{58}$; and (d),(h) $Zn_{83}Se_{83}$. The horizontal dashed lines mark the values for the neutral atoms, i.e., 12 for Zn and 6 for Se.

arrange into separate bands as it was found for other II-VI semiconductor clusters. The bands corresponding to selenium $4s$ functions lies in the range between -17.5 and -16.5 eV, the one corresponding to Zn $3d$ in the range -11 to -10 eV, and the uppermost occupied band between -8.5 to -5.5 eV is formed mainly due to the Se $4p$ and partly by Zn $4s$ functions. Apart from the fact that for the larger clusters the bands are slightly broader, the other features are remarkably similar. Our results are in qualitative agreement with earlier theoretical studies on related semiconductor clusters.[46–50] Another important observation that the effects of structural relaxation (see the shift of Fermi energy) is more pronounced for wurtzite cluster than the zinc-blende clusters.

The optoelectronic properties of semiconductor nanoparticles are dominated by excitonic effects, in particular by the
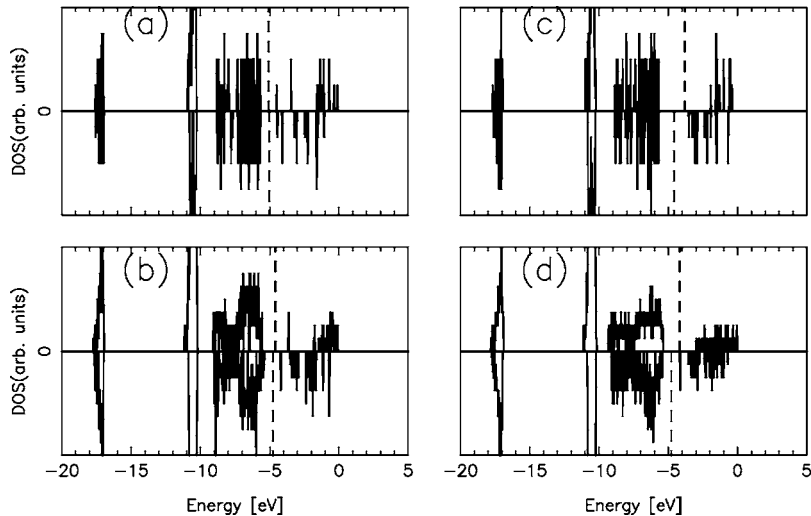

FIG. 4. Density of states (DOS) for different zinc-blende (left column) and wurtzite-derived (right column) clusters of different sizes: (a),(c) $Zn_{16}Se_{16}$ and (b),(d) $Zn_{83}Se_{83}$. The upper part of each panel is representing relaxed and the lower part unrelaxed structures, respectively. The vertical dashed lines mark the Fermi energy. Notice that the different panels have different scales on the y axis.
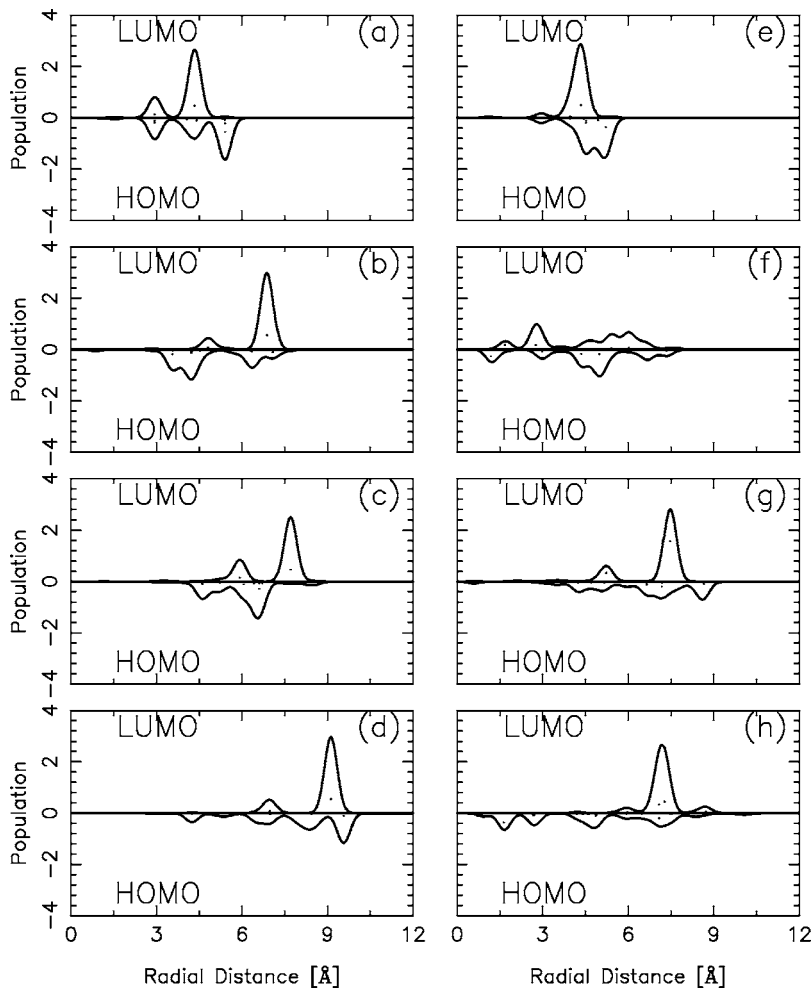
FIG. 5. The schematic representation of the radial distribution of the HOMO and the LUMO for zinc-blende (left column) and wurtzite-derived clusters (right column) of different sizes: (a),(e) $Zn_{16}Se_{16}$; (b),(f) $Zn_{37}Se_{37}$; (c),(g) $Zn_{58}Se_{58}$; and (d),(h) $Zn_{83}Se_{83}$.

recombination of the electron-hole pairs forming the excitons. To a first approximation the excitonic wave function is determined by the orbitals closest to the gap, i.e., the HOMO and the LUMO, and the relaxation processes will, therefore, depend strongly on the spatial distribution of these orbitals. In order to arrive at a qualitative description of the distribution of the various orbitals, we define a radial density as follows. With N_{ij} being the Mulliken gross population for the jth atom and ith orbital we define the following density:

$$\rho_i(\vec{r}) = \sum_j N_{ij}\left(\frac{2\alpha}{\pi}\right)^{3/2}\exp[-\alpha(\vec{r}-\vec{R}_j)^2]. \qquad (4)$$

Here, N_{ij} is the Mulliken gross population for the jth atom and ith orbital and α being a chosen, fixed constant. Subsequently, we calculate the spherical average of this density, which is the one shown in Fig. 5. From the figure it is seen that for small clusters (e.g., $Zn_{16}Se_{16}$ both zinc-blende and wurtzite structures) both HOMO and LUMO are localized on the surface, but as the cluster size increases HOMO is delocalized through out the whole cluster and LUMO is localized at the surface. The delocalization of HOMO throughout the whole cluster is more pronounced for wurtzite clusters. There is also experimental evidence for the surface localization of the LUMO. Bawendi *et al.*[54] observed that one or both charge carriers of the exciton are trapped and localized

on the surface. Analyzing the two orbitals in more detail, we found that the LUMO has dominating contributions from the outer Zn atoms. As LUMO is the surface state, its energy depends sensitively on the cluster surface. Moreover, the surface localization of the LUMO has the consequence that HOMO and LUMO has different spatial distribution within the cluster. This difference in spatial distribution of HOMO and LUMO is important for low energy transitions and is in agreement with the recent experimental results of Lifshtiz *et al.*[55,56] on related CdSe clusters.

The sensitivity of the LUMO to surface variation can be identified in Fig. 5 (upper half) in which we have plotted the HOMO and LUMO energies as a function of the cluster size for zinc-blende (left panel) and wurtzite structures (right panel). The results show that the dependence of energy of the HOMO on cluster size is smooth whereas the same for LUMO is irregular and oscillating which is a clear indication that the HOMO being delocalized over the complete cluster and the LUMO being a surface state for the cluster size studied here. For zinc-blende clusters the variation of HOMO energy with the cluster size is not as smooth as that we found for wurtzite clusters. This also supports our observation that for zinc-blende clusters the delocalization of the HOMO through out the whole cluster are not pronounced.

The lower part of Fig. 6 shows the variation in the total energy (dashed curve) as well as HOMO-LUMO energy gap
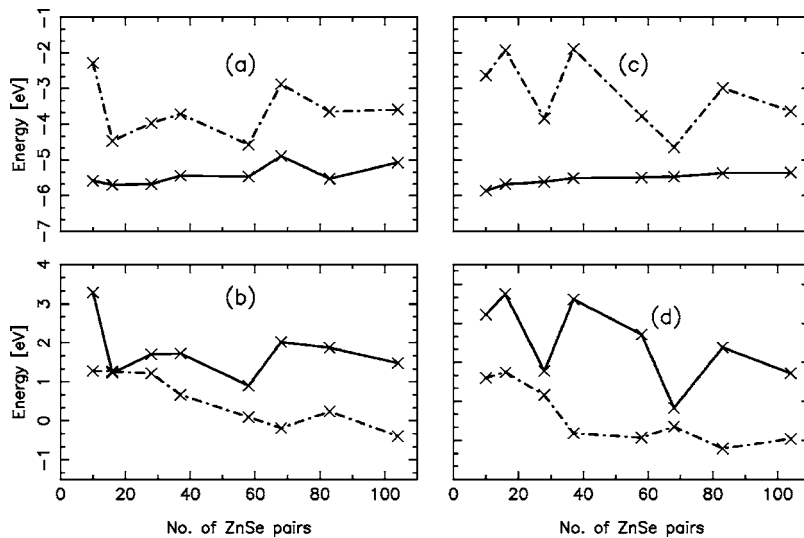
FIG. 6. (a),(c) HOMO (solid curve) and LUMO (dashed curve) energies as well as (b),(d) HOMO-LUMO gap (solid curve) and relative total energy per ZnSe pair (shifted by an additive constant) (dashed curve) for stoichiometric zinc-blende (left column) and wurtzite derived clusters (right column) as functions of the number of ZnSe pairs.

(solid) per ZnSe pair. The HOMO-LUMO gap for the infinite crystals are 2.363 and 2.304 eV for zinc-blende and wurtzite structures, respectively. From the figure it is seen that there is an overall increase in the band gap with decreasing nanocrystal size for both zinc-blende and wurtzite clusters. However the increase is not a monotonic function of the cluster size. In our earlier studies with other II-VI semiconductor systems we observe a marked correlation between the energy gap and the total energy; low total energy (large stability) correlates with large HOMO-LUMO gap. This finding may actually be considered related to the [hard and soft acids and bases (HSAB)] principle;[57] systems are particularly inert (stable) if their hardness is particularly large. As a first approximation, the hardness is simply the HOMO-LUMO en-
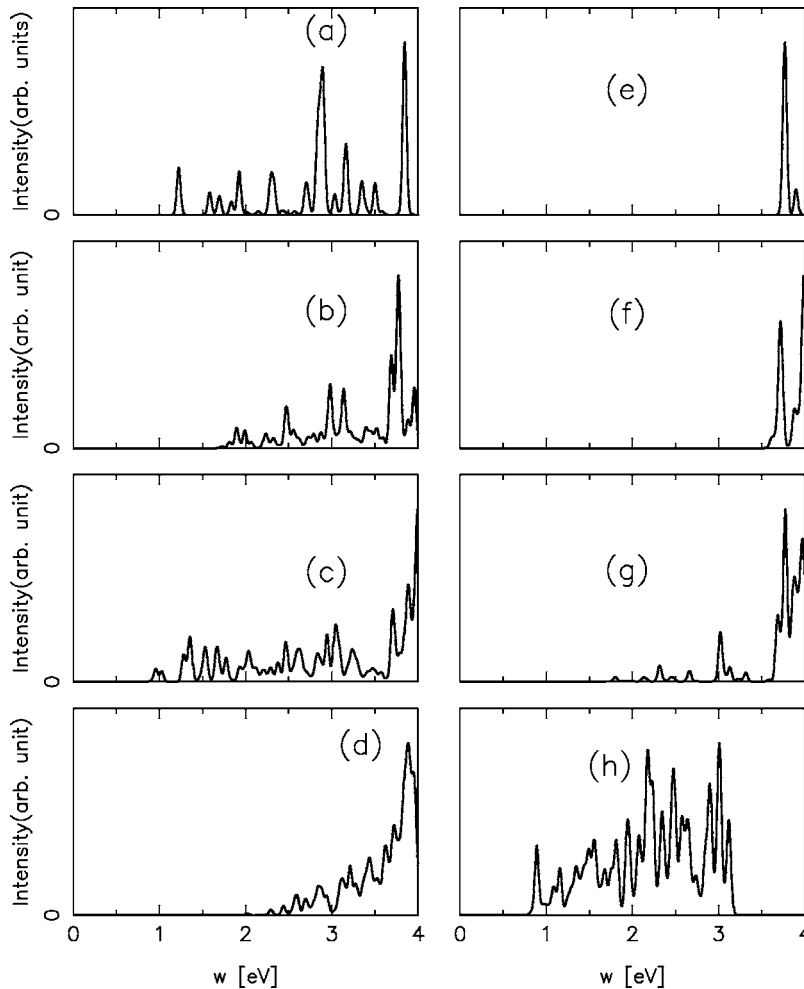

FIG. 7. TD-DFRT-TB spectra of zinc-blende (left column) and wurtzite (right column) derived ZnSe clusters of different size: (a),(e) $Zn_{16}Se_{16}$; (b),(f) $Zn_{37}Se_{37}$; (c),(g) $Zn_{58}Se_{58}$; and (d),(h) $Zn_{68}Se_{68}$. (All y axes have the same scale, and all curves are broadened with Gaussians 0.27 eV.)
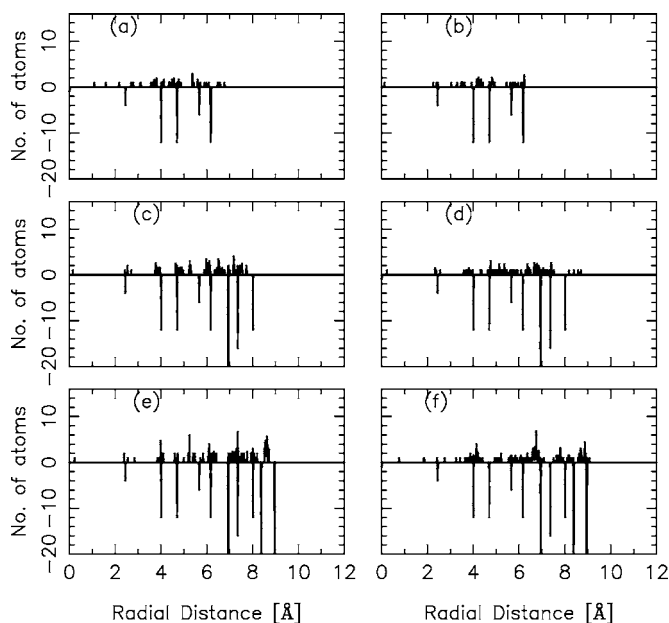
FIG. 8. Radial distribution of Zn and Se atoms for nonstoichiometric Zn-rich (left column) and Se-rich (right column) clusters of different sizes: (a) $Zn_{28}Se_{19}$, (c) $Zn_{55}Se_{44}$, (e) $Zn_{79}Se_{68}$, (b) $Zn_{19}Se_{28}$, (d) $Zn_{44}Se_{55}$, and (f) $Zn_{68}Se_{79}$. The upper part of each panel represents relaxed and the lower part unrelaxed structures, respectively.
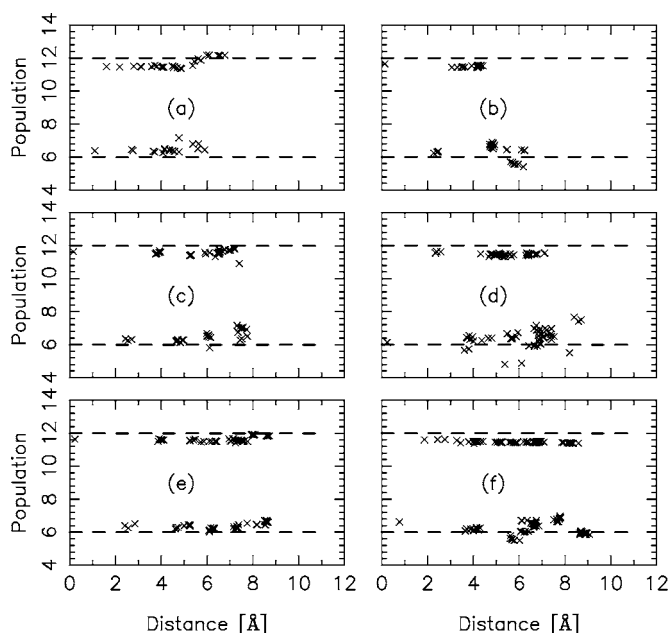

FIG. 9. Radial distribution of Mulliken gross populations for the nonstoichiometric clusters of different size and composition: (a) $Zn_{28}Se_{19}$, (c) $Zn_{55}Se_{44}$, (e) $Zn_{79}Se_{68}$, (b) $Zn_{19}Se_{28}$, (d) $Zn_{44}Se_{55}$, and (f) $Zn_{68}Se_{79}$. The upper part of each panel represents relaxed and the lower part unrelaxed structures, respectively. The dashed lines correspond to the populations of the neutral atoms, i.e., 12 for Zn and 6 for Se.

ergy gap. For the ZnSe clusters there is also such correlation between band gap and the energy, but a careful inspection of the figure reveals that the correlation is not as sharp as we observed for other II-VI clusters. The fact that the band gap of ZnSe nanocrystal increases with decreasing nanocrystal size is in agreement with the recent experimental work on ZnSe QDs.[30] Although the band gap value increases with decreasing nanocrystal size the values are not much large as expected because of quantum confinement effects. These low value may be explained from the presence of surface states from the single bonded surface atoms in the cluster. As LUMO are the surface states and the major contribution to LUMO comes from the outer Zn atoms, then the surface passivation with the ligand [e.g., TOPO(tri octyl phosphine oxide), through oxygen atoms] which binds Zn atoms will increase the band gap.

Electronic excitations as computed with time-dependent (TD) density-functional response theory (DFRT) for eight different clusters are shown in Fig. 7. The interesting feature of the figure is the variation of the lowest excitation energies for different size clusters. From the figure it is evident that the most of the wurtzite clusters have higher lowest excitation energies than the corresponding zinc-blende clusters. And the lowest excitation energy shows a clear blueshift for wurtzite clusters (right panel of the figure) when the size of the cluster is reduced. Therefore, the main crystal structure has strong influence on the absorption spectrum of a cluster, particularly on the magnitude of HOMO-LUMO gap. A close inspection of the optimized structure of these clusters reveals that the magnitude of the lowest excitation energy depends very much on the number of single bonded atoms in the cluster. In Table I we compare the lowest excitation energies

(gap) with the number of single bonded atoms in the cluster. The correlation of lowest excitation energies and number of single bonded atoms is easily established. The clusters with no single bonded atoms has HOMO-LUMO gap around

TABLE I. Excitation energies (gap) and number of single bonded atoms. The first column displays the structure (Z for zinc-blende and W for wurtzite) and the number of ZnSe pairs per cluster, the second column contains the calculated lowest excitation (by TD-DFRT-TB) and the last column displays the number of single-bonded surface atoms.

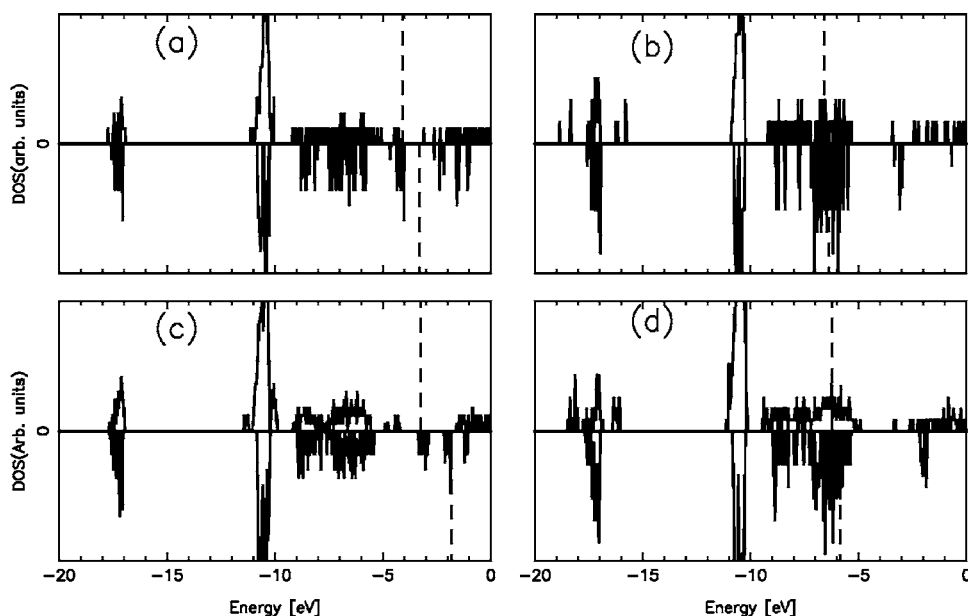| Number of ZnSe pairs	gap[eV]	Number of single bonded atoms
Z10	3.293	0
Z16	1.227	6
Z37	1.727	6
Z43	3.310	0
Z58	0.90	6
Z65	3.762	0
Z68	2.018	3
Z83	1.876	6
W10	3.223	0
W16	3.751	0
W38	3.615	0
W57	2.714	2
W69	0.827	14
W81	2.382	0

FIG. 10. Density of states for the nonstoichiometric clusters of two different sizes: (a) $Zn_{28}Se_{19}$, (c) $Zn_{79}Se_{68}$ and (b) $Zn_{19}Se_{28}$, (d) $Zn_{68}Se_{79}$. The upper part of each panel is representing relaxed and the lower part unrelaxed structures, respectively. The dashed vertical lines correspond to fermi level. Notice that the different panels have different scales on the y axis.

3 eV which is higher than bulk ZnSe and other clusters having single bonded atoms have a much lower HOMO-LUMO gap. This feature is independent of the crystal structure, i.e., whether it is zinc-blende or wurtzite. Joswig *et al.* have observed the same on related CdS clusters. Finally, the magnitude of the band gap of ZnSe nanocrystals (having no single bonded atoms) are in good agreement with experimental values of Smith *et al.*[30] (around 3.5 eV).

B. Nonstoichiometric clusters

Most experimentally synthesized clusters are nonstoichiometric in nature. So we extend our study to some nonstoichiometric ZnSe clusters. In studying the nonstoichiometric
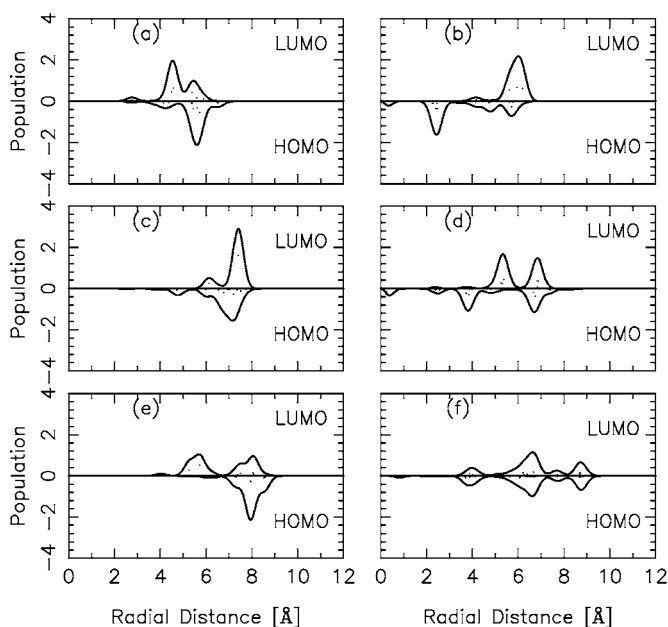

FIG. 11. Schematic representation of the radial distribution of HOMO and the LUMO of nonstoichiometric clusters of different size and composition: (a) $Zn_{28}Se_{19}$, (c) $Zn_{55}Se_{44}$, (e) $Zn_{79}Se_{68}$, (b) $Zn_{19}Se_{28}$, (d) $Zn_{44}Se_{55}$, and (f) $Zn_{68}Se_{79}$.

clusters, we only considered those derived from the zinc-blende crystal structure. For the unrelaxed stoichiometric clusters of the preceding subsection, the surfaces contained in all cases the same number of Zn and Se atoms, whereas in the present case the surface is formed exclusively by one type of atoms. Considering a spherical part of a general AB zinc-blende crystal with the center at an A atom, the next layer will contain 4 B atoms, then 12 A atoms, followed by 24 atoms, then 6 A atoms, and 12 B atoms, followed by 24 atoms and so on. This gives clusters with stoichiometric A, AB_4, $A_{13}B_4$, $A_{13}B_{16}$, $A_{19}B_{16}$, $A_{19}B_{28}$, $A_{43}B_{28}$,…, which are alternating A and B rich as well as alternately terminated by A and B atoms. Subsequently, we apply the same method in relaxing the structure of the clusters to its nearest total-energy minimum.

Due to the differences in the stoichiometries it is not obvious how to compare the total energies of different nonstoichiometric clusters. Therefore, no such comparison is presented. Instead we proceed by analyzing the radial distribution of atoms and of the Mulliken gross populations.

In Fig. 8 we have shown the radial distribution of the atoms for the six representative systems. It is clearly seen that for these clusters the effects of relaxation are extended throughout the major parts of the clusters. Almost all atoms are found to change their positions significantly. The Mulliken gross populations are shown in Fig. 9. Compared to the stoichiometric clusters, the identification of a surface layer characterized by a large electron transfer between Zn and Se not very clear. For these nonstoichiometric clusters where the outermost atoms are of the only one type, the tendency of the chalcogen atoms to move outward and of the metal atoms to move in wards upon structural relaxation, as found for stoichiometric clusters, are also recovered here. This is clearly seen in the figure: the left-hand panels for the Zn-rich clusters are simultaneously the clusters with Zn atoms as the outermost atoms before relaxation. These clusters possess an overall contraction. On the other hand, for the Se-rich clusters with Se atoms as the outermost clusters, i.e., the right-hand panels, the cluster expand.

Both for the Zn and Se rich clusters the HOMO-LUMO gap is small compared to stoichiometric cluster which is very clear in density of state figures (Fig. 10). The fact that the HOMO-LUMO gap for the nonstoichiometric clusters is smaller than that of the stoichiometric clusters is in agreement with the experimental results of Kolenbrander and Mandich.[58] Finally, in Fig. 11 we have shown the schematic representation of the radial distribution of HOMO and LUMO. For Zn-rich clusters (left panel) both HOMO and LUMO are located on the same atoms and they are both surface states. But for Se-rich clusters the spatial distribution of HOMO and LUMO shows strong size dependence.

IV. CONCLUSIONS

We have calculated the electronic structure as a function of the nanocrystallite size for Zn_mSe_n semiconductor using the DFTB method. To the best of our knowledge, this work represents the first systematic study of the structural, electronic and optical properties of both zinc-blende and wurtzite modification of stoichiometric ZnSe cluster and also nonstoichiometric ZnSe clusters of zinc-blende modification. The studies of both radial distribution and Mulliken population identifies a surface region of 2.5–3.5 Å thickness essentially independent of the size of the cluster. In the outer region of the cluster there is transfer of two electrons from Zn to Se implying that within this surface region the inter atomic bonds have a larger ionic character than the interior of the cluster where they are largely covalent. The band gap increases with the decrease in particle size but the decrease is not monotonic as it is found in other studies. We found a correlation between band gap and stability, however, the correlation is not sharp as we found for other II-VI semiconductor clusters. Similar to other II-VI semiconductor cluster, e.g., CdS, CdSe, for ZnSe clusters also the HOMO is delocalized over the whole cluster, whereas, the LUMO is localized in the surface region in agreement with the experimental observation of Bawendi et al.[54] A detailed analysis of the orbital population of HOMO and LUMO suggests that the HOMO has the major contribution from the surface Se atoms whereas the LUMO has the major contributions from the outer Zn atoms. As LUMO has the major contributions from the surface Zn atoms, then the surface passivation with the ligand that binds the metal atom will increase the band gap. By using time-dependent density-functional response theory with tight-binding approximation we have calculated electronic excitation energies for different size clusters. We have found that the low band gap value is because of the surface states arises from the single bonded surface atoms. We have also reported some results on nonstoichiometric Zn_mSe_n clusters. For nonstoichiometric clusters the band gap are low compared to the stoichiometric clusters. The frontier orbitals (both HOMO and LUMO) for these clusters are localized on the surface atoms. Finally, it would be very interesting to see how the ligand that passivates the dangling bonds present on the surface modifies the optical properties of ZnSe nanocrystals, since this will allow for meaningful comparison of the calculated and observed properties.

*E-mail address: pranab_69@yahoo.co.in

[1] C. N. R. Rao, G. U. Kulkarni, P. J. Thomas, and P. P. Edwards, Chem.-Eur. J. **8**, 28 (2002).

[2] J. R. Heath, J. J. Shiang, Chem. Soc. Rev. **27**, 65 (1998).

[3] A. P. Alivisatos, J. Phys. Chem. **100**, 13226 (1996).

[4] S. H. Tolbert and A. P. Alivisatos, Annu. Rev. Phys. Chem. **46**, 595 (1995).

[5] M. R. Hoffman, S. T. Martin, W. Choi, and D. W. Bahnemann, Chem. Rev. (Washington, D.C.) **95**, 69 (1995).

[6] A. Henglein, in *Topics in Current Chemistry* (Springer, Berlin, 1988), Vol. 143.

[7] A. D. Yoffe, Adv. Phys. **42**, 173 (1993).

[8] M. Nirmal, D. J. Norris, M. Kuno, M. G. Bawendi, A. L. Efros, and M. Rosen, Phys. Rev. Lett. **75**, 3728 (1995).

[9] S. Gorer, G. Hodes, in *Semiconductor Nanoclusters*, edited by P. V. Kamat and D. Meisel (Elsevier Science, Amsterdam, 1996).

[10] M. Schlamp, X. Peng, and X. A. P. Alivisatos, J. Appl. Phys. **82**, 5837 (1997).

[11] M. Bruchez, M. Morronne, P. Gin, S. Weiss, and A. P. Alivisatos, Science **281**, 2046 (1998).

[12] W. Huynh, X. Peng, and A. P. Alivisatos, Adv. Mater. (Weinheim, Ger.) **11**, 923 (1999).

[13] N. Cheatnoy, T. D. Harris, R. Hull, and L. E. Brus, J. Phys. Chem. **90**, 3393 (1986).

[14] V. L. Kolvin, M. C. Schlamp, and A. P. Alivisatos, Nature (London) **370**, 354 (1994).

[15] D. L. Klein, R. Roth, A. K. L. Lim, A. P. Alivisatos, and P. L. McEuen, Nature (London) **389**, 699 (1997).

[16] A. P. Alivasatos, Science **271**, 933 (1996).

[17] J. Hu, L.-S. Li, W. Yang, L. Manna, L.-W. Wang, and A. P. Alivisatos, Science **292**, 2060 (2001).

[18] L.-S. Li, J. Hu, W. Yang, and A. P. Alivisatos, Nano Lett. **1**, 349 (2001).

[19] C. B. Murray, D. J. Norris, and M. J. Bawendi, J. Am. Chem. Soc. **115**, 8706 (1993).

[20] C. B. Murray, C. R. Kagan, and M. G. Bawendi, Science **270**, 1335 (1995).

[21] H. Weller, Angew. Chem., Int. Ed. Engl. **35**, 1079 (1996).

[22] T. Y. Tsai and M. Birnbaum, J. Appl. Phys. **87**, 25 (2000).

[23] H. Ishikura, T. Abe, N. Fukuda, and K. Ando, Appl. Phys. Lett. **76**, 1069 (2000).

[24] K. Katayama, H. Yao, F. Nakanishi, H. Doi, A. Saegusa, N. Okuda, and T. Yamada, Appl. Phys. Lett. **73**, 102 (1998).

[25] M. Kuhnelt, T. Leichtner, S. Kaiser, B. Hahn, H. P. Wagner, D. Eisert, G. Bacher, and A. Forchel, Appl. Phys. Lett. **73**, 584 (1998).

[26] Z. H. Ma, W. D. Sun, and G. K. L. Won, Appl. Phys. Lett. **73**, 1340 (1998).

[27] D. Sarigiannis, J. D. Peck, G. Kioseoglou, A. Petrou, and T. J. Mountziaris, Appl. Phys. Lett. **80**, 4024 (2002).

[28] T. Tawara, S. Tanaka, H. Kumano, and I. Suemune, Appl. Phys. Lett. **75**, 235 (1999).

[29] H. Rho, H. E. Jackson, S. Lee, M. Dobrowolska, and J. K. Furdyna, Phys. Rev. B **61**, 15641 (2000).

[30] C. A. Smith, H. W. H. Lee, V. J. Leppert, and S. H. Risbud, Appl. Phys. Lett. **75**, 1668 (1999).

[31] B. Xiang, H. Z. Zhang, G. H. Li, F. H. Yang, F. H. Su, R. M. Wang, J. Xu, G. W. Lu, X. C. Sun, Q. Zhao, and D. P. Yu, Appl. Phys. Lett. **82**, 3330 (2003).

[32] G. N. Karanikolos, P. Alexandridis, R. Mallory, A. Petrou, and T. J. Mountziaris, Nanotechnology **16**, 2372 (2005).

[33] S. L. Cumberland, K. M. Hanif, A. Javier, G. A. Khitrov, G. F. Strouse, S. M. Woessner, and C. S. Yun, Chem. Mater. **14**, 1576 (2002).

[34] P. Deglmann, R. Ahlrichs, and K. Tsereteli, J. Chem. Phys. **118**, 1585 (2002).

[35] L.-W. Wang and A. Zunger, Phys. Rev. B **53**, 9579 (1996).

[36] A. Mizel and M. L. Cohen, Phys. Rev. B **56**, 6737 (1997).

[37] K. Eichkorn and R. Ahlrichs, Chem. Phys. Lett. **288**, 235 (1998).

[38] N. A. Hill and K. B. Whaley, J. Chem. Phys. **100**, 2831 (1994).

[39] A. Tomasulo and M. V. Ramkrishna, J. Chem. Phys. **105**, 3612 (1996).

[40] L.-W. Wang and A. Zunger, J. Phys. Chem. B **102**, 6449 (1998).

[41] K. Leung, S. Pokrant, and K. B. Whaley, Phys. Rev. B **57**, 12291 (1998).

[42] M. C. Troparevsky and J. R. Chelikowsky, J. Chem. Phys. **114**, 943 (2001).

[43] D. Porezag, Th. Frauenheim, Th. Kohler, G. Seifert, and R. Kaschner, Phys. Rev. B **51**, 12947 (1995).

[44] G. Seifert, D. Porezag, and Th. Frauenheim, Int. J. Quantum Chem. **58**, 185 (1996).

[45] T. A. Niehaus, S. Suhai, F. Della Sala, P. Lugli, M. Elstner, G. Seifert, and Th. Frauenheim, Phys. Rev. B **63**, 085108 (2001).

[46] J.-O. Joswig, M. Springborg, and G. Seifert, J. Phys. Chem. **104**, 2617 (2000).

[47] J.-O. Joswig, S. Roy, P. Sarkar, and M. Springborg, Chem. Phys. Lett. **365**, 75 (2002).

[48] S. Roy and M. Springborg, J. Phys. Chem. B **107**, 2771 (2003).

[49] P. Sarkar and M. Springborg, Phys. Rev. B **68**, 235409 (2003).

[50] S. Pal, B. Goswami, and P. Sarkar, J. Chem. Phys. **123**, 044311 (2005).

[51] *Semiconductor Physics of II-VI Compounds*, edited by K. H. Hellwege, Vol. 17 of Landolt-Bornstein, New Series, Group-III, Pt. B (Springer, Berlin, 1982).

[52] J.-O. Joswig, G. Seifert, T. A. Niehaus, and M. Springborg, J. Phys. Chem. B **107**, 2897 (2003).

[53] M. G. Bawendi, M. L. Steigerwald, and L. E. Brus, Annu. Rev. Phys. Chem. **41**, 477 (1990).

[54] M. G. Bawendi, W. L. Wilson, L. Rothberg, P. J. Carroll, T. M. Jedju, M. L. Steigerwald, and L. E. Brus, Phys. Rev. Lett. **65**, 1623 (1990).

[55] E. Lifshitz, I. Dag, I. Litvin, and G. Hodes, J. Phys. Chem. **102**, 9245 (1998).

[56] E. Lifshitz, I. Dag, I. Litvin, G. Hodes, S. Gorer, R. Reisfeld, M. Zelner, and H. Minti, Chem. Phys. Lett. **288**, 188 (1998).

[57] R. G. Pearson, *Chemical Hardness* (Wiley-VCH, Weinheim, Germany, 1997).

[58] K. D. Kolenbrander and M. L. Mandich, Phys. Rev. Lett. **65**, 2169 (1990).